The conserved nature of nitrogen recycling within the bacterial pouch of *Tetraponera* ants

Mingjie Ma[1], Biru Zhu[1], Dayong Zhang[1], Piotr Łukasik[2], Yi Hu[1]

1. Ministry of Education Key Laboratory for Biodiversity Science and Ecological Engineering, College of Life Sciences, Beijing Normal University, Beijing 100875, China
2. Institute of Environmental Sciences, Faculty of Biology, Jagiellonian University, Kraków, Poland

Abstract

Microbial symbioses are fundamental to the nutrition of many animal groups, yet the mechanisms of nutrient recycling have only been characterized in a few social insect systems. Here, we investigate the functional significance of a specialized and unusual symbiotic organ—the bacterial pouch—in four ant species within the *Tetraponera nigra*-group, focusing on the symbionts' roles in nitrogen recycling and colony fitness. This unique organ houses a microbial community consistently dominated by the co-diversifying bacterial symbiont *Tokpelaia*, occasionally accompanied by other stable bacterial associates. Metagenomic sequencing and targeted ^{15}N-labeled urea feeding experiments demonstrate that these symbionts assimilate nitrogen from urea (likely derived from uric acid) and transfer it to adult workers and developing larvae, incorporating recycled nitrogen into host tissues. Disruption of this symbiosis severely impairs larval growth and overall colony fitness. Overall, our study highlights the critical role of the bacterial pouch in sustaining colony fitness in nitrogen-limited environments, providing new insights into the co-evolutionary dynamics between insect hosts and their microbial partners.

Keywords:

microbiome, microbiota, bacteriome, amino acid biosynthesis, Formicidae

Introduction

The symbiotic relationships have significantly influenced ecological dynamics and evolutionary trajectories of interacting multicellular organisms and their microbiota. Notably, the associations formed between specific microbial partners and dedicated host organs play a critical role in shaping these interactions. Classic examples include plant root nodules, which harbor nitrogen-fixing rhizobia[1, 2], and the light organs of bobtail squid[3, 4], home to bioluminescent bacteria. Similarly, mycangia in ambrosia beetles[5] serve as reservoirs for fungal symbionts, while specialized gut organs in bean bugs[6] and bacteriomes in many Hemiptera insects[7, 8] provide a habitat for nutrient-provisioning bacteria. Despite the importance of symbiont-hosting organs, our understanding of their diversity and distribution across various phylogenetic lineages and the specificity and ecological significance of host-microbe associations remains notably incomplete.

Ants (Hymenoptera: Formicidae) are among the most ecologically successful and significant groups of insects on Earth. Their mutualistic interactions with microbes have been identified as an important factor driving their long-term evolution and ecological dominance[9, 10, 11, 12]. Recent studies have shown that several ant groups harbor diverse microbial communities that influence multiple life history traits of their ant hosts[10, 13]. In particular, microbes' abilities to provide essential nutrients such as amino acids, vitamins, and other metabolic byproducts that ants cannot synthesize themselves are considered a key driver that enables ants to thrive in various nutrient-imbalanced niches, contributing to their widespread ecological dominance[11, 14, 15, 16, 17].

A remarkable pattern in ant evolution is multiple shifts from nitrogen-rich carnivory and omnivory to nitrogen-poor herbivory. Herbivorous ants typically scavenge for foods such as honeydew from tended sap-feeding insects, extrafloral nectar, pollen, fungi, and plant wound secretions[18, 19, 20]. The availability of accessible nitrogen and essential amino acids in these food sources is typically limited. The

relatively high occurrence of specialized bacteria in herbivorous ant taxa indicates that they may often rely on microbial partners to mitigate nitrogen limitation and nutritional imbalance[10, 11, 12, 13]. Recent studies using high-throughput sequencing and functional assays have shown a trend of functional convergence in nitrogen recycling capabilities among symbionts of unrelated herbivorous ants that feed on N-poor or N-inaccessible foods. Such nitrogen provisioning by symbionts has been demonstrated in carpenter ants (genus *Camponotus*), whose intracellular symbiont *Blochmannia* synthesizes essential amino acids from recycled nitrogen for their hosts[21, 22]. In the herbivorous ant tribe Cephalotini, analogous roles fulfilled by abundant, conserved multi-species bacterial communities present within the gut lumen were both predicted from metagenomic data and demonstrated *in vivo* and *in vitro*[17, 23]. In the herbivorous genus *Dolichoderus*, the same functions were predicted based on metagenomic data but not demonstrated experimentally[16].

Due to the intricate social structure of ant colonies, the nutritional demands of their colony members differ significantly. Larvae require substantial protein intake for their rapid growth, and adult workers, with their higher carbohydrate needs for energy[24], have distinct dietary needs. This dietary divergence proposes a greater challenge for ant larvae in obtaining sufficient nitrogen than adult workers. The critical role of symbiotic bacteria in the overall nutrition of ant colonies has been well studied in *Camponotus* ants, which harbor intracellular symbionts *Blochmannia* at all developmental stages. It was shown that antibiotic-treated colonies suffered from a decline in the number of larvae developing into pupae, smaller body size of newly eclosed workers, and reduced overall colony sizes[25], highlighting the essential role that *Blochmannia* plays in supporting colony development through its impact on nitrogen balance and brood nutrition. In contrast, extracellular symbionts associated with ants are typically restricted to specific life stages. Their role in nutrition supplementation across the entire colony and their broader impact on colony-wide nutrition and development remains an area that requires further investigation.

The arboreal ant genus *Tetraponera*, restricted to the Palaeotropics and Australia, encompasses approximately 110 described species divided into six distinct species

groups[26, 27] that were shown to vary in their nutritional biology and anatomy[28, 29, 30]. The *T. nigra*-group, comprising 20 species, is uniquely characterized by an unusual bacterial pouch located at the junction between the midgut and hindgut. This pouch is connected to Malpighian tubules and the tracheal system and is densely populated with bacteria[31]. This structure bears a resemblance to the symbiotic organs observed in other insects such as leaf beetles[32], bean bugs[33], or ambrosia beetles[5], but also with root nodules of legumes[1], suggesting that these ants engage in a specialized form of nutritional symbiosis with microbial partners[34]. Stable isotopic analysis revealed that *T. nigra*-group ants are at a relatively low trophic level (Fig. 1B). Indeed, three species in the group, *T. tucurua*[35], *T. binghami*[30, 36], and *T. punctulata*[35], have been documented feeding on honeydew produced by scale insects, and one species *T. rotula*[37] feeding on extrafloral nectar – foods considered nutritionally imbalanced. We hypothesized that the nutritional symbiosis with specialized microorganisms housed within gut pouches may have enabled these ants to occupy ecological niches where essential nutrients are otherwise scarce, providing a potential explanation for the success of this group in such habitats. Hence, in a broad sample spanning multiple colonies of several species, we anticipated finding evidence for the symbiosis stability, the conservation and expression of symbiont functions related to nitrogen recycling and nutrient biosynthesis, and a correlation between symbiosis disruption and colony health.

The goal of this study was to comprehensively characterize the diversity and functional roles of bacterial symbionts and their significance in the nutritional biology of the *T. nigra*-group ants. We first asked about the general organization of the gut structure in connection with the bacterial pouch across ant life stages. Second, we characterized the diversity of microbial communities within bacterial pouches across colonies of four species and the phylogenetic position and genomic characteristics of the dominant bacteria. Third, we assessed the roles of these symbiotic bacteria in nutrient metabolism, with an emphasis on nitrogen recycling and provisioning. Lastly, we explored how they contribute to nutritional supplementation for the entire colony, particularly for larvae. We addressed these questions by combining microscopic

analysis, 16S rRNA gene amplicon sequencing, metagenomics, and *in vivo* colony feeding experiments. Through this multi-pronged investigation, we demonstrated how specialized symbiotic relationships underpin the nutritional ecology of these herbivorous ants.

Results

T. nigra-group ant workers have evolved an unusual organ – bacterial pouch

Previous studies have revealed the presence of a pouch-like structure in the gut of adult workers from three *T. nigra*-group ant species[31]. Our microscopy analyses of the four ant species from the *T. nigra*-group, including two previously characterized[31] (*T. attenuata*, *T. binghami)* and two newly identified and so far undescribed (*T.* sp1 and *T.* sp2 - Fig. 1A and Supplementary Fig. 1), confirmed that this specialized gut structure is consistently present within the group. In adult workers of four ant species, this pouch-like structure is located at the junction between the midgut and hindgut and is connected to several Malpighian tubules (Fig. 1C, I-L). The inner lining of the pouch lumen consists of microvillar cells containing numerous mitochondria, and a dense population of rod-shaped bacteria enclosed by a double membrane are housed inside the pouch (Fig. 1F and G). The whole-mount fluorescence in situ hybridization (FISH) reveals that bacteria are concentrated within the pouch-like structure in all four ant species (Fig. 1I-L), confirming its role as a symbiotic organ, referred to as the bacterial pouch in the *T. nigra*-group ants.

When comparing across life stages of *T. nigra*-group ants, scanning electron microscopy observations revealed that larvae lack the specialized bacterial pouch (Fig. 1E), which only develops during the pupal stage (Fig. 1D). The symbiotic organ in the pupal stage is underdeveloped compared to that of adults: smaller in size and not yet fully swollen. Furthermore, the results from the transmission electron microscopy

showed a notable absence of bacteria in the symbiotic organ during the pupal stage (Fig. 1H). This indicates that the establishment of symbiotic relationships occurs after worker eclosion.

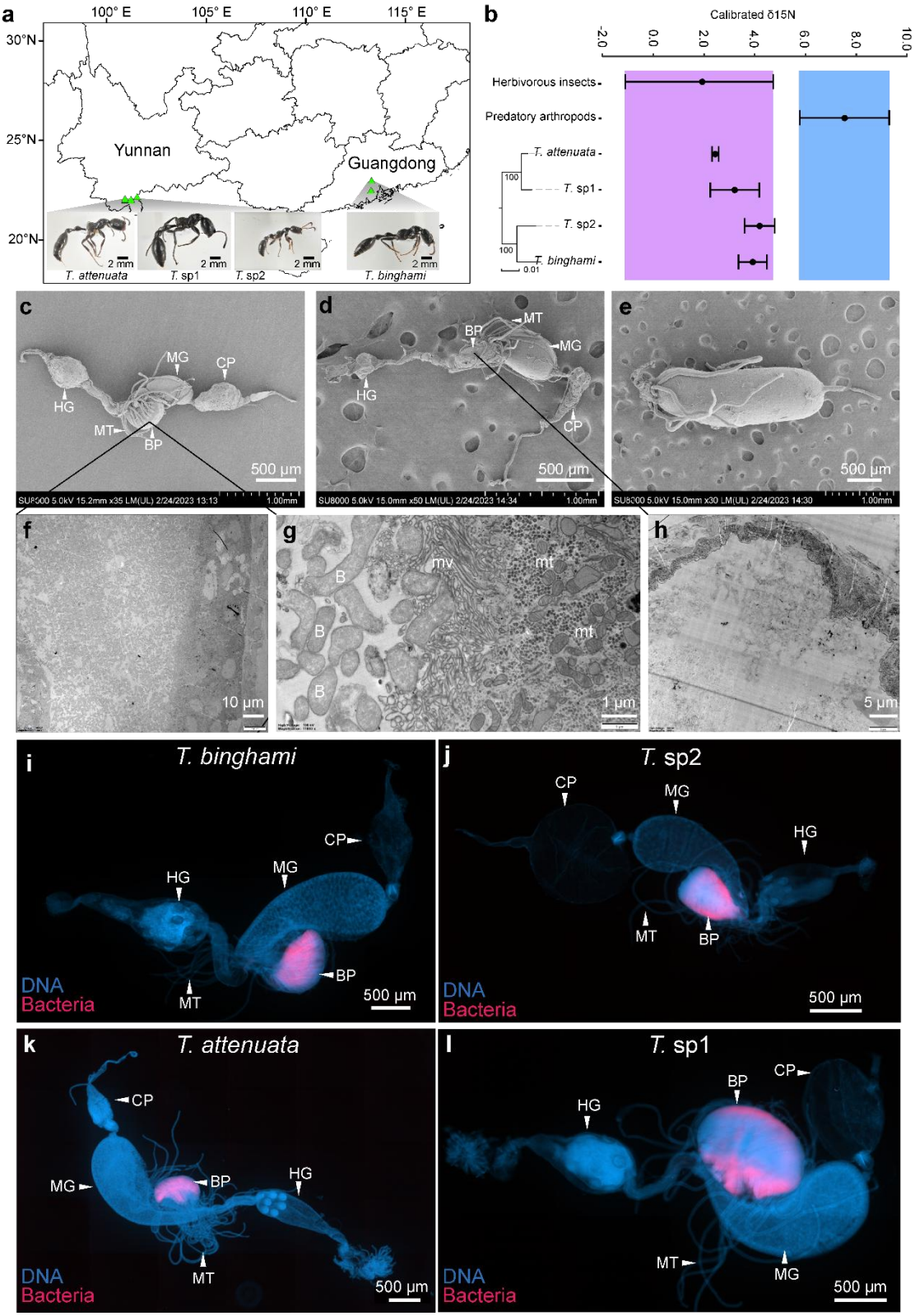

Fig. 1 Origins of specimens and gut structure of the *T. nigra*-group ants. **(a)** Sampling locales for four ant species used in this study (image credit: Mingjie Ma). **(b)** Nitrogen isotope ratios utilized to assess the trophic levels of four species. Shown are the mean and standard deviation of nitrogen isotope ratios for four *Tetraponera* ant species and herbivorous (purple box) and predatory (blue box) insects from the same site. The bottom side displays a phylogeny of the four ant species based on 1329 single-copy orthologs. **(c-e)** Scanning electron microscope (SEM) images showing the gut structure of *T. attenuata* at different developmental stages: worker, pupa, and larva. **(f-h)** TEM images of ultrathin sections illustrating the bacteria within the bacterial pouch of *T. attenuata* at worker (with different magnifications) and pupal stage, respectively. **(i-l)** Fluorescence in situ hybridization (FISH) detection of symbiotic bacteria within the bacterial pouch of four *Tetraponera* ant species. DNA and bacteria are denoted by blue and magenta, respectively. CP, crop; MG, midgut; MT, Malpighian tubules; BP, bacterial pouch; HG, hindgut; B, bacteria; mv, microvillar differentiation; mt, mitochondria.

Microbiota of *T. nigra*-group ants are consistently dominated by pouch-associated Hyphomicrobiales bacteria

16S rRNA amplicon sequencing for dissected gasters of replicate workers from four to six colonies from each of the four *T. nigra*-group species revealed striking consistency in bacterial communities (Fig. 2, Supplementary Data 4). In all species, the microbiota was predominantly composed of a single OTU assigned to the order Hyphomicrobiales (formerly Rhizobiales), representing 99.4–100% of all reads in *T. attenuata*, 98.7–99.9% in *T.* sp1, 61.1–96.9% in *T. binghami*, 77.1–99.9% in *T.* sp2. Each ant species harbored a single distinct Hyphomicrobiales zOTU. In addition, we identified an OTU representing unclassified members of the Alphaproteobacteria class in three species. One of these zOTUs was present in all individuals of *T.* sp1 and *T.* sp2, and the other was found in all individuals of *T. binghami.* Despite consistent presence, their relative abundance was relatively low (e.g., 0.06–3.4% in *T.* sp2, 0.1–1.1% in *T.* sp1, 0.3–11.5% in *T. binghami*). Furthermore, we found that all *T. binghami* individuals hosted an additional zOTU from the order Xanthomonadales, with relative abundances ranging from 1.4% to 27.7%. All other bacterial zOTUs combined comprised an average of 0.13% of reads in a library (ranging from 0 to 2.55%).

We used fluorescence in situ hybridization, with probes specific to each Hyphomicrobiales zOTU to localize them in ant guts. The signal overlapped with that for broad-spectrum bacterial probes – confirming that Hyphomicrobiales fill up the bacterial pouch (Fig. 2).

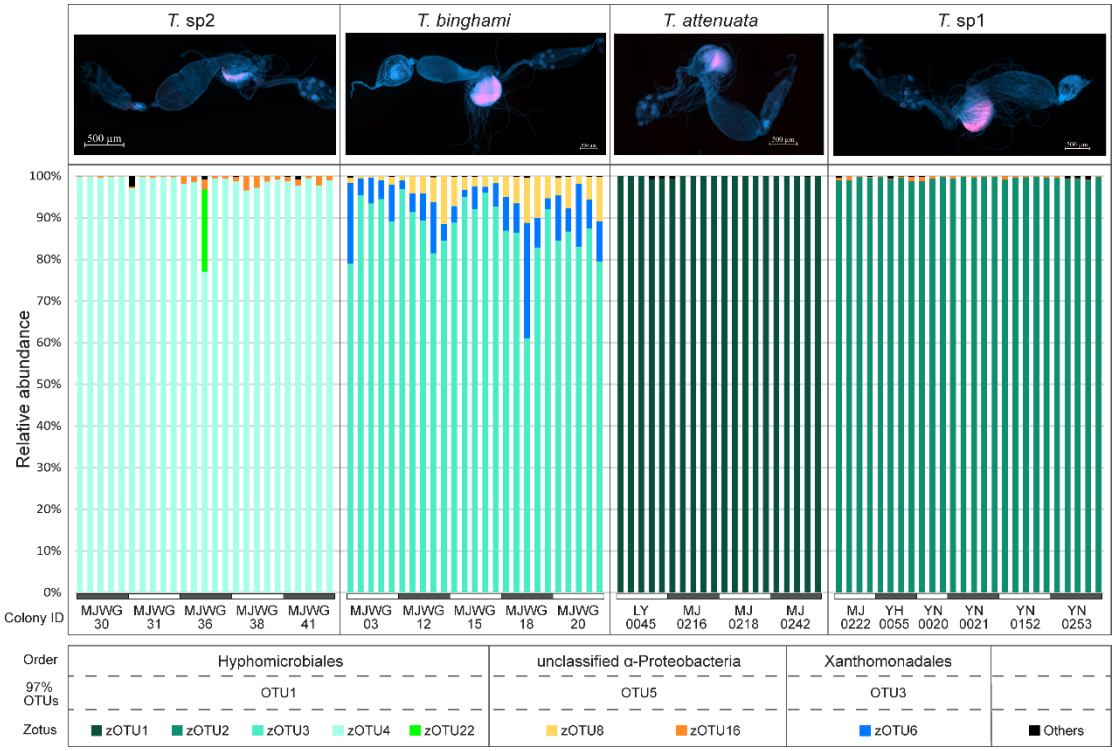

Fig. 2 Symbiont diversity and the localization of dominant Hyphomicrobiales bacteria within the gut of workers from four *T. nigra*-group species. The bar graphs show the relative abundance of bacterial zOTUs across individual workers from replicate colonies of four ant species. zOTUs with a relative abundance of less than 1% in any sample and the prevalence of less than 80% occurrence in any ant species are summed up as "others". ZOTUs were clustered into operational taxonomic units (OTUs) with 97% similarity. Above the bar graphs, fluorescence in situ hybridization (FISH) results illustrate the localization of Hyphomicrobiales bacteria within the worker ants' guts. Blue, DAPI; Red, Hyphomicrobiales-specific probe.

Comparative genomics reveals conserved symbiont lineages in the *T. nigra*-group

After sequencing metagenomes for pooled worker guts from the four *T. nigra*-group species, we performed metagenomic binning to generate draft symbiont genomes, all with more than 90% completeness and less than 1% contamination from the gut microbiomes of four ant species (Supplementary Table 3). The draft genome classification through comparison with the Genome Taxonomy Database aligned with the 16S rRNA amplicon-based findings (Fig. 3A). Specifically, all *Tetraponera* species hosted a dominant and unique Hyphomicrobiales strain. Additionally, *T. binghami* and *T.* sp1 were found to carry an unclassified Alphaproteobacteria strain, while *T. binghami* uniquely possessed a distinct Xanthomonadales strain.

The draft genomes of Hyphomicrobiales strains from the four ant species ranged

201 in size between 1.18 and 1.26 Mb, with an average GC content from 47.4% to 49.5%.
202 The maximum likelihood phylogeny based on a concatenated alignment of 385 amino
203 acid sequences of single-copy orthologous genes confirmed that the four *Tetraponera*
204 symbionts grouped together and formed a distinct, well-supported monophyletic clade,
205 along with other ant-associated Hyphomicrobiales symbionts with sequenced genomes
206 (Fig. 3B). This ant-associated bacterial clade forms a sister group to the *Bartonella*
207 clade, which includes *B. apis* of honeybees and pathogenic *Bartonella* species. This
208 result is also supported by the phylogenetic tree constructed based on 16S rRNA
209 sequences (Supplementary Fig. 2). Intriguingly, the phylogenomic relationships among
210 bacterial strains did not fully agree with the phylogeny of their ant hosts: strains from
211 *T. attenuata* and *T.* sp1 were not identified as sister clades, unlike their hosts. Further,
212 genome organization comparisons revealed that despite multiple rearrangements, there
213 are large areas of synteny among *T. nigra*-group symbiont genomes – much more so
214 than relative to *Tokpelaia* genomes from other ants (Supplementary Fig. 5). The 16S
215 rRNA gene identities and the average amino acid identities in all pairwise comparisons
216 between all ant-associated Hyphomicrobiales symbionts were 94.61%-97.91% and
217 62.33%-97.23% (Supplementary Table 4), respectively, suggesting that they should be
218 considered as members of the same genus *Tokpelaia*. Thus, we proposed to consider
219 the *Tetraponera nigra* group symbionts as strains of a single species, *candidatus*
220 Tokpelaia tetraponerae.

221 Our 16S rRNA gene phylogeny (Supplementary Fig. 2) indicated that the *T. nigra*-
222 group associated with unclassified Alphaproteobacteria and Xanthomonadales
223 symbionts were each grouped into a well-supported *Tetraponera*-specific clade,
224 respectively. Metagenomic binning further revealed the genomic characteristics of
225 these symbiont bacteria. The two unclassified Alphaproteobacteria strains had genomes
226 of approximately 1.13 Mb with a GC content of 27.4% (Supplementary Table 3).
227 Phylogenetic analysis placed them within the order Holosporales (Supplementary Fig.
228 3), a group known to include obligate intracellular or intranuclear symbionts of
229 protists[38, 39]. In addition, the Xanthomonadales bacterium, found exclusively in *T.*
230 *binghami*, had a genome size of 2.36 Mb and a GC content of 60.99% (Supplementary

Table 3). Phylogenetic analysis revealed its close relationship with 100% bootstrap support to *Frateuria aurantia* isolated from the lily plant *Lilium auratum.* However, taxonomic inconsistencies within the *Frateuria* genus preclude precise genus-level assignment, and thus, we provisionally classify it within the Rhodanobacteraceae family. While this last symbiont has the largest genome among the symbionts of *T. nigra*-group ants, it is still significantly reduced compared to the closely related bacteria (Supplementary Fig. 3).

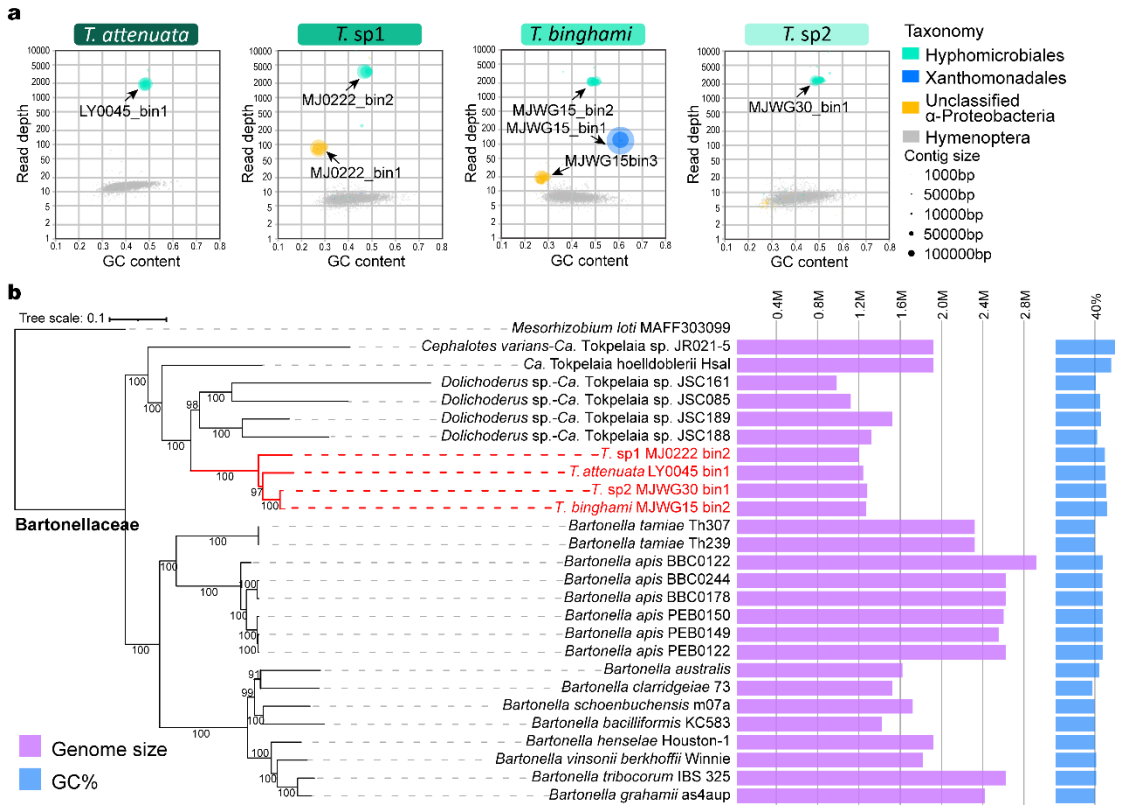

Fig. 3 Taxon-annotated GC-coverage plots for four *Tetraponera* metagenomes and phylogenetic relationships of dominant Hyphomicrobiales bacteria of *T. nigra*-group ants and other hosts. (a) Assembled scaffolds in each metagenome are plotted based on their %GC content (x-axis) and their depth of sequencing coverage (y-axis, log scale). The colors of the blob plots indicate the taxa to which the scaffolds were assigned. Circle size represents the length of each scaffold. Scaffolds assigned to unclassified organisms are not shown. (b) Phylogenomic tree generated by maximum likelihood analysis based on 385 homologous single-copy genes. Red branches represent the Hyphomicrobiales genomes obtained from the metagenome of four *T. nigra*-group ant species. The purple bars represent the genome size, and the blue bars represent the GC content.

Nitrogen recycling and provisioning facilitated by the *T. nigra*-group ant symbionts

Given that the diets of these ants are deficient in nitrogen, yet their symbionts reside in a bacterial pouch enriched with nitrogenous waste such as uric acid delivered through the Malpighian tubules, we proposed that these symbionts likely convert nitrogenous waste into forms usable for synthesizing amino acids required by the ant host. Analysis of *Tokpelaia* genomes supports this hypothesis, as they retained genes encoding enzymes involved in nitrogen cycling from nitrogenous waste and biosynthetic pathways for the production of most essential amino acids that are needed by the ant hosts (Fig. 4).

All the *Tokpelaia* genomes harbored the *uacT* gene, which encoded a transporter for uric acid—the primary metabolic waste transported by the host's Malpighian tubules into the bacterial pouch. Further, all *Tokpelaia* strains contain gene clusters encoding enzymes involved in all the uric acid degradation pathway steps except for the last (Fig. 4). Interestingly, the missing gene, *alc*, which encodes allantoicase that converts allantoate to urea, is ancestrally lost in ant-associated *Tokpelaia* strains (Supplementary Fig. 10). This gene is present on Hymenoptera-assigned scaffolds in metagenomes of the *T. nigra*-group ants except *T.* sp1, suggesting that this reaction is likely carried out by the ant hosts. Following uric acid degradation, the product urea could be further processed into ammonia through the urease, encoded by three core genes, *ureC*, *ureB,* and *ureA* (Supplementary Data 7), present in all sampled metagenomes. Further, all *Tokpelaia* strains possess the genes *gdhA* and *glnA*, encoding enzymes glutamate dehydrogenase (GDH) and glutamine synthetase (GS), respectively (Fig. 4). These enzymes assimilate ammonia incorporated from urease-driven urea degradation into glutamate and glutamine, which serve as the nitrogen donors for the biosynthesis of amino acids.

The *Tokpelaia* genomes retain complete pathways for the biosynthesis of essential amino acids, including phenylalanine, tryptophan, tyrosine, arginine, lysine, threonine,

277 and methionine (Fig. 4, Supplementary Fig. 8). The isoleucine, leucine, and valine
278 pathways are nearly complete, although *ilvH* gene encoding the small subunit of
279 acetolactate synthase is missing. It is possible that these reactions are catalyzed by the
280 large subunit (*ilvB*) of acetolactate synthase alone in *Tokpelaia,* as demonstrated in
281 some Enterobacteria intact[40] enzymes.

282 Despite their specialized role in nitrogen metabolism, the four *Tokpelaia* strains
283 exhibit striking metabolic constraints. While retaining genes for core cellular processes,
284 including translation, replication, and transcription, their metabolic gene repertoire is
285 notably limited (Supplementary Figs. 6-9). The symbionts' genomes lacked key genes
286 involved in glycolysis, the biosynthesis of most B vitamins, certain non-essential amino
287 acids, nucleotides, and KDO_2-lipid A. However, the metabolic pathways of these
288 symbionts remain intact for the TCA cycle, oxidative phosphorylation, the biosynthesis
289 of peptidoglycan, and fatty acids. Notably, the primary metabolic functions contributed
290 by these symbionts are nitrogen recycling and provisioning, which account for
291 approximately 12% of all protein-coding genes (Supplementary Fig. 7, Supplementary
292 Data 7).

293 Analysis of the Xanthomonadales genome uniquely found in *T. binghami* revealed
294 its metabolic redundancy, as it harbored genes encoding enzymes involved in ammonia
295 assimilation and the biosynthesis of most amino acids (Fig. 4). Particularly, while genes
296 *ilvH* and *hisB* were missing from across all examined *Tokpelaia* genomes, both were
297 present in the Xanthomonadales genomes. In contrast, Holosporales strains lack
298 biosynthetic pathways for almost all amino acids (Fig. 4, Supplementary Fig. 8), but
299 encode transporters for oligopeptides and several amino acids. In addition, they also
300 harbor glucose PTS transporters encoded by ptsG, enabling glucose to serve as the
301 substrate fueling their TCA cycle (Supplementary Data 7). Like other Holosporales
302 bacteria reported previously[41, 42], these bacteria are unlikely to be involved in ant
303 nutrition, despite their strikingly consistent presence.

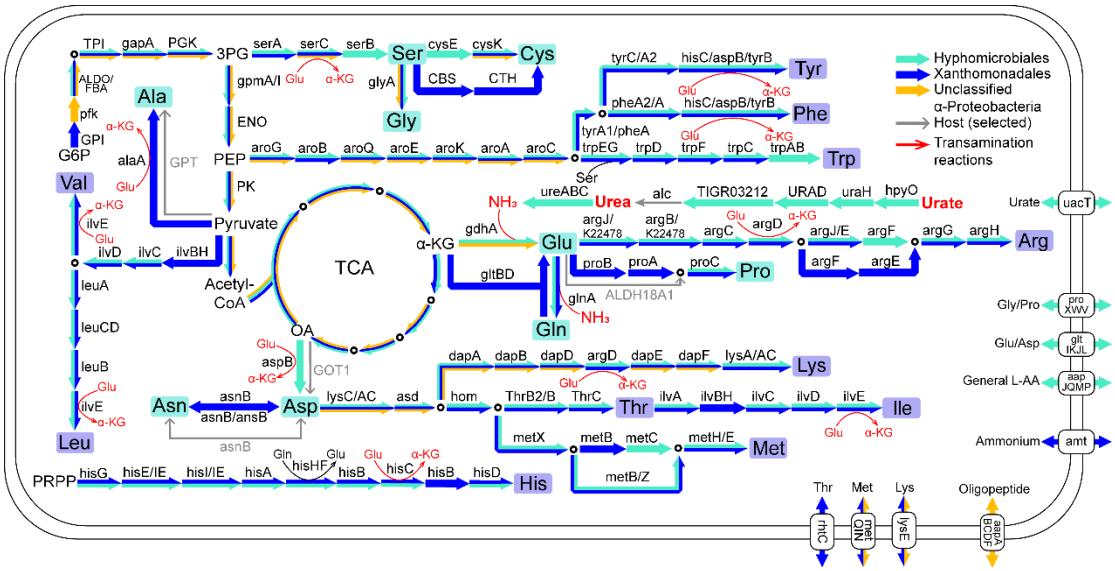

Fig. 4 Amino acid biosynthetic and nitrogen (N) cycle utilization genes and pathways in the genomes of *Tetraponera* ants-related symbionts. The distinct colors of the arrows represent the genomes of different symbiotic bacteria or hosts. Please note that this figure does not annotate the entire metabolic symbiosis of the host; only the steps crucial to the nitrogen cycle pathway are highlighted

Microbiota disruption negatively affects colony-wide fitness

Given the metagenomic evidence for nutritional provisioning by pouch-associated symbionts, we assessed the symbiont impact on host survivorship and development. We first generated symbiont-free workers by removing pupae from the original colonies to sterile dishes. Those isolated pupae kept under sterile conditions emerged as adult workers with no bacteria in the bacterial pouch, confirmed by universal bacterial PCRs, as well as *Tokpelaia*-targeted 16S rRNA gene PCRs and whole-mount FISH staining (Supplementary Fig. 11).

We then compared fitness parameters between the two groups of larvae with similar sizes: one reared by normal workers (Sym-workers) and the other reared by symbiont-free, aposymbiotic workers (Apo-workers), in two ant species, *T. attenuata* and *T.* sp1. Through detailed daily observation of the larval development status over a 30-day period, we observed that larvae tended by symbiont-free workers in both species exhibited significantly lower survivorship (Fig. 5A; Wald statistic = 192.6, $p < 2e\text{-}16$ for *T.* sp1; Wald statistic = 180.6, $p < 2e\text{-}16$ for *T. attenuata*) and slower development, as indicated by reduced body length (Fig. 5B; $\chi^2 = 897.982$, $p < 2.2e\text{-}16$ for *T.* sp1; $\chi^2 = 721.6$, $p < 2.2e\text{-}16$ for *T. attenuata*; GLMM) compared to larvae reared by normal

workers.

In another long-term experiment lasting 90 days, we monitored the continuous development of the larvae until they emerged as adults. After 90 days, the number of missing broods was higher in the group tended by symbiont-free workers compared to the one reared by normal workers only in *T. attenuata* (Fig. 5C, Supplementary Table 8; $p = 0.0848$; t-test). In both ant species, we observed that larvae raised by symbiont-free workers exhibited significantly lower pupation rates (Fig. 5C, Supplementary Table 8; *T.* sp1, $p = 0.0096$; *T. attenuata*, $p = 0.2326$; T-test), reduced adult emergence rates from pupae to adults (Fig. 5C, Supplementary Table 8; *T.* sp1, $p = 0.1999$, Wilcoxon-Mann-Whitney test; *T. attenuata*, $p = 0.2271$, t-test), as well as smaller head widths at the time of emergence (Fig. 5C, Supplementary Table 8; *T.* sp1, $p = 0.1818$, Wilcoxon-Mann-Whitney test; *T. attenuata*, $p = 0.0453$, t-test), compared to those reared by normal workers. We also noted that among the adult ants tending the larvae, symbiont-free workers exhibited significantly lower survivorship compared to their symbiont-bearing counterparts (Supplementary Fig. 13; Wald statistic = 94.22, $p < 2e-16$ for *T.* sp1; Wald statistic = 3.44, $p = 0.06$ for *T. attenuata*).

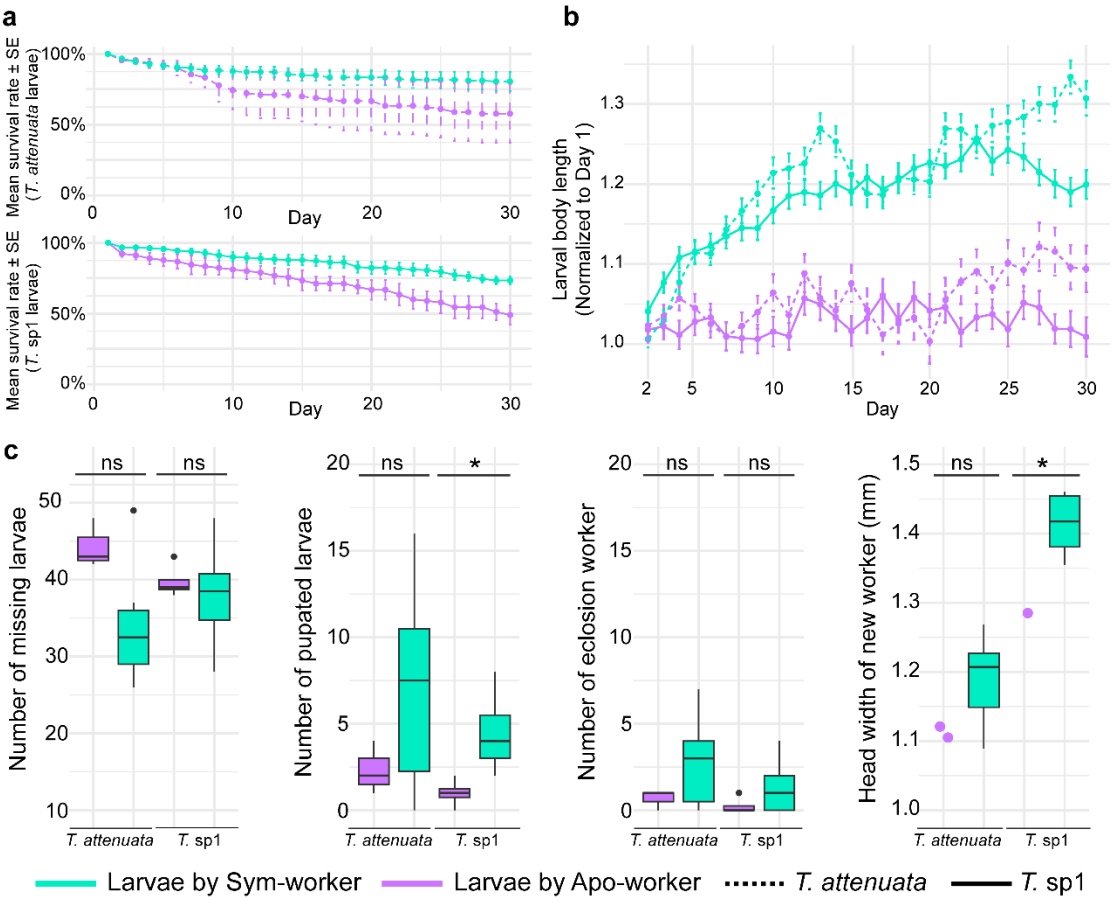

Fig. 5 Comparison of fitness parameters between two groups of larvae with similar sizes, one reared by normal workers (Sym-workers) and the other reared by symbiont-free workers (Apo-workers), in two ant species, *T. attenuata* and *T.* sp1. (a) The survival rate of larvae cared for by Apo-workers or Sym-workers over a 30-day experimental period. **(b)** Changes in the relative body length of larvae reared by Sym-workers and Apo-workers. Body length data from day 2 to day 30 were normalized to the average body length of larvae on day 1 for each treatment group. **(c)** Comparison of fitness parameters at day 90, including the number of missing larvae, pupation rate, eclosion rate, and head width of newly emerged workers as an indicator of body size. The light green color represents the control group of worker ants with symbiotic bacteria, while the purple indicates the experimental group of worker ants without symbiotic bacteria. In the line graphs, the dashed lines represent *T. attenuata*, and the solid lines represent *T.* sp1.

Symbionts help ants recycle nitrogen from urea

To experimentally test whether genetic signatures reflect the abilities of symbionts to degrade nitrogenous wastes and synthesize amino acids, we conducted feeding experiments with ^{15}N-labelled urea (Supplementary Fig 12) to two species from the *T. nigra*-group. Within each ant colony, individuals were assigned to one of three experimental groups: (1) symbiotic workers fed ^{15}N-labelled urea; (2) symbiont-free workers fed ^{15}N-labelled urea; and (3) symbiont workers fed ^{14}N-labelled urea as a control.

363 In the first experiment, we focused exclusively on workers. We examined whether
364 recycled nitrogen from ^{15}N-labelled urea could be incorporated into the free amino
365 acids present in the hemolymph of adult ants. Among symbiotic workers fed with ^{15}N-
366 urea, we detected a significantly higher proportion of ^{15}N in 14 of 19 measurable amino
367 acids compared to the control group fed diets containing only standard urea (significant
368 p-value range: 1.04E−05 to 0.076, Fig. 6A, Supplementary Table 9). These enriched
369 amino acids included seven essential amino acids (arginine, histidine, isoleucine,
370 phenylalanine, tryptophan, tyrosine, and valine), as well as seven non-essential amino
371 acids (alanine, asparagine, glutamate, glutamine, glycine, proline, and serine). Crucially,
372 this heavy isotopic enrichment was dependent on symbiont presence. Symbiont-free
373 workers fed ^{15}N-labelled urea showed no such enrichment in the same amino acids
374 relative to the ^{14}N-labelled urea fed control ants. These results highlighted the pivotal
375 role of bacterial pouch symbionts in recycling nitrogen, particularly in facilitating
376 amino acid synthesis essential to the host.

377 In the second experiment, we investigated how symbiotic bacteria within the
378 bacterial pouch of workers mediate nitrogen allocation to larvae, given the severe
379 negative effects of worker microbiota disruption on larval growth and development (Fig.
380 5). By tracking ^{15}N incorporation from ^{15}N-urea into the amino acids of larval body
381 tissue, we found that larvae reared by symbiotic workers fed ^{15}N-urea exhibited ^{15}N
382 enrichment in 11 amino acids of 18 measurable amino acids (significant p-value range:
383 0.001 to 0.0861, Fig. 6B, Supplementary Table 10). In contrast, larvae tended by either
384 symbiont-free workers (^{15}N-urea fed) or symbiotic workers (^{14}N-urea fed) showed no
385 such enrichment. Among these 11 enriched amino acids, there are nine essential amino
386 acids (arginine, histidine, isoleucine, leucine, lysine, phenylalanine, tryptophan,
387 tyrosine, and valine) and two non-essential amino acids (glycine and serine). This
388 highlights the worker symbionts' role in bridging nutritional needs critical for larval
389 growth and development.

390 To evaluate how symbiont-processed nitrogen is allocated among members within
391 the whole colony, the relative incorporation of ^{15}N into worker and larval tissues was
392 quantified. We observed that δ^{15}N values in the body tissues of larvae attended by

symbiotic workers for 30 days were significantly higher compared to those reared by aposymbiotic workers in two ant species (*T. attenuata*, p=0.0373; *T.* sp1, p=0.0399; post hoc Dunn's test; Supplementary Fig. 14, Supplementary Table 11). Similarly, $\delta^{15}N$ values in the body tissues of symbiotic workers were higher than those of aposymbiotic workers (*T. attenuata*, p = 0.1062; *T.* sp1, p = 0.1052; post hoc Dunn's test; Supplementary Fig. 14, Supplementary Table 11). Notably, comparative analysis revealed that larvae exhibited 2.2-fold and 2.3-fold higher ^{15}N enrichment compared to symbiotic workers tending them in *T. attenuata* and *T.* sp1 respectively (*T. attenuata*, p = 0.0022; *T.* sp1, p = 0.0005; t-test). These findings reflected this larval-biased nitrogen allocation as an adaptive investment strategy, where colonies prioritize developmental stages to maximum fitness under N-limiting conditions.

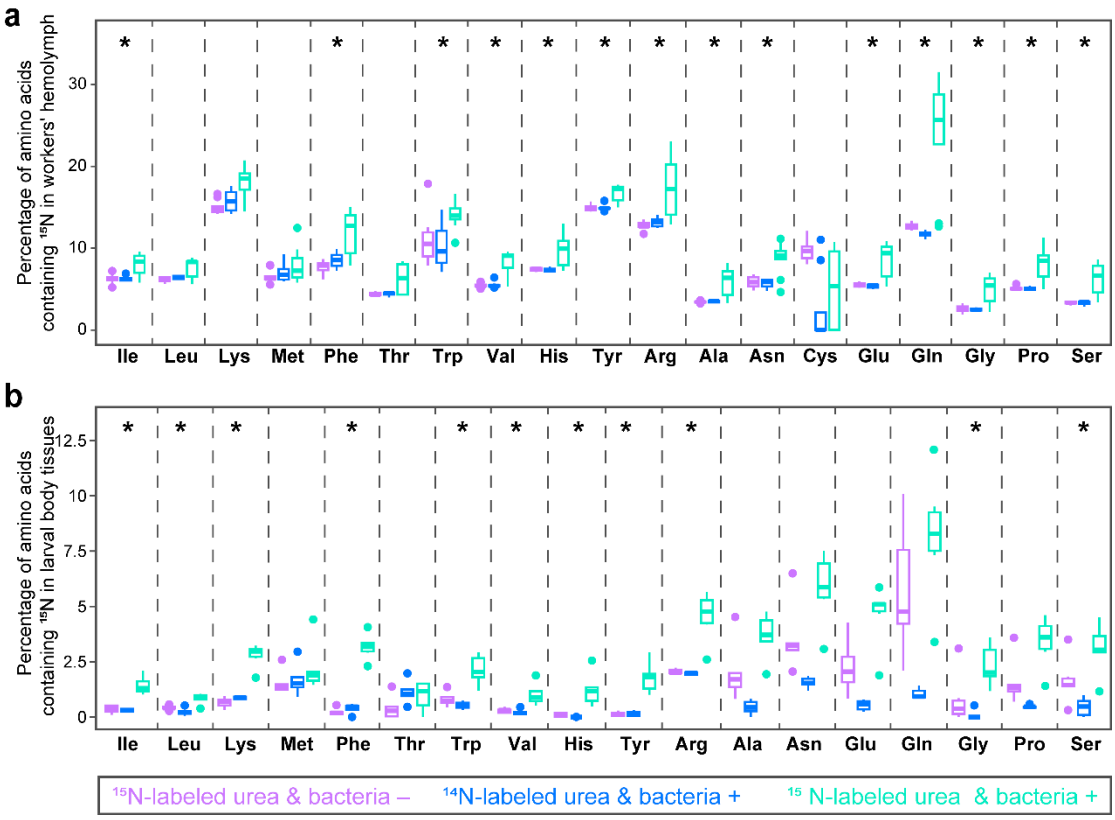

Fig. 6 Depriving symbiotic bacteria reduces the proportion of ^{15}N-labeled amino acids in the worker ants and larvae that have consumed ^{15}N-labeled urea. (a) The proportion of ^{15}N-labeled amino acids in the hemolymph of *T. attenuata* workers was measured under three conditions: symbiotic workers fed ^{15}N-labeled urea, symbiont-free workers fed ^{15}N-labeled urea, and symbiotic workers fed ^{14}N-labeled urea as a control. Detailed information on sample sizes for each treatment can be found in Supplementary Data 10. The statistical results are described in Supplementary Methods and Supplementary Table 9. **(b)** The proportions of ^{15}N-labeled amino acids in the body tissues of larvae cared for by workers of *T. attenuata* and *T.* sp1 under the same three conditions. Due to limited sample size per species (n=3 under one condition) and non-significant interspecific effect on the proportion of ^{15}N amino acids (Supplementary Table 11), data from two species were

pooled across group for a combined analysis using one-way ANOVA (for normally distributed data) or Kruskal Wallis test (for non-normal data).

Discussion

Our study has demonstrated the unique location of symbiotic bacteria within a gut pouch (Fig. 1H-1K), a special structure consistently present across the *T. nigra*-group. We also demonstrated for the first time the ants' ancestral symbioses with a co-diversifying *Tokpelaia* symbiont, while also maintaining consistent associations with some other bacteria (Figs. 2 and 3). Through the characterization of the symbionts' genomic characteristics, we have elucidated the mechanisms underlying this nutritional symbiosis (Fig. 4). Additionally, we have demonstrated experimentally the effects of symbiosis disruption on colony development, particularly highlighting the impact on larval growth (Fig. 5). Finally, we have experimentally established links between symbiont genomic characteristics and ant nutrition, explaining the observed fitness effects (Fig. 6). Considering the diversity, global distribution, and ecological importance of social insects, it is surprising how few clades and species have comparably detailed data on microbial associations. Through this study, the *T. nigra*-group ants are added to the short list of social insect clades whose symbioses are considered well-understood.

The *T. nigra*-group is distinguished by a unique bacterial pouch—a structure not previously reported in other hymenopteran clades—highlighting an unconventional method of symbiont localization. In contrast, other hymenopteran insects exhibit diverse anatomical niches for hosting symbiotic bacteria. For instance, *Blochmannia* is found in bacteriocytes situated between midgut cells and in female ovaries[43, 44]; species such as honeybees[45, 46], bumblebees[47], turtle ants[17, 48], and army ants[49] harbor multi-partite bacteria within their guts; and fungus-farming ants maintain bacterial communities in specialized exoskeletal crypts essential for the health of their fungal gardens[50]. However, several other groups of insects, including stinkbugs[51] and leaf beetles[32, 52], host extracellular bacteria in a symbiotic organ consisting of pouch-like gut

444 invagination. These symbiotic organs ensure a stable supply of resources for the
445 symbiotic bacteria, which promoting their growth while limiting competition with other
446 microbial species[53]. Meanwhile, these structures restrict the entry of symbionts into
447 other host tissues, minimizing disruption to the hosts' other physiological processes[53].

448 We observed that the larvae of *T. nigra*-group ants lack a bacterial pouch (Fig. 1E).
449 Although the pouch first develops during the pupal stage (Fig. 1D), it remains
450 uncolonized (Fig. 1H) until the ants eclose into adults (Fig. 1C). This indicated that this
451 symbiotic organ develops independently of symbiont colonization. A similar pattern of
452 organ development, proceeding without symbiont triggering, has been observed in
453 tortoise beetles, reflecting an ancient evolutionary trait in which the formation of such
454 organs proceeds autonomously[54]. Moreover, pupae isolated from their colony and
455 allowed to eclose in isolation showed no bacterial colonization of their pouch
456 (Supplementary Fig. 15), suggesting that symbiotic bacteria are likely transmitted to
457 newly emerged adults through trophallactic interactions within the colony. Such
458 trophallaxis behaviors may play a key role in maintaining partner fidelity, not only in
459 these groups of ants but also across several other social insects. For instance, symbionts
460 are transmitted between termite siblings via oral-anal trophallaxis[55], and a similar
461 transmission mode has been observed in *Cephalotes* and *Procryptocerus* ants[56]. In
462 honeybees, gut symbiotic bacteria are transmitted through a combination of trophallaxis
463 or contact with nest materials within the hive[57]. Future investigation of transmission
464 mechanisms of symbiotic bacteria in the bacterial pouch can shed light on key drivers
465 of co-diversification between the *T. nigra*-group ants and their symbiotic bacteria.

466 High-throughput sequencing revealed an ant-specific, *Tokpelaia*-dominated
467 bacterial community in the *T. nigra*-group ants' pouch, suggesting a specialized and
468 long-standing association between the *T. nigra*-group ants and their symbiotic bacteria.
469 Our conclusions are further strengthened by the phylogenetic similarity between the
470 symbionts characterized here and those previously generated from other *T. nigra*-group
471 species[58, 59]. Our findings suggest that the *T. nigra*-group ants belong to a growing
472 number of insect clades whose extracellular microbiota are dominated by one or a few

specialized symbionts—a pattern similarly observed in other insect groups with specialized symbiotic organs, such as stinkbugs[7] and leaf beetles[32, 60, 61]. One possible explanation is that these symbiotic organs function to filter microbial strains, allowing only specific symbionts to access the host and maintain a beneficial partnership. This contrasts with the complex multi-partite gut microbiota observed in termites[62, 63], *Cephalotes* ants[17], and corbiculate bees[46], or with occasional and non-specialized microbial association seen in diverse other ants and other insects[64].

The critical role of symbiotic bacteria in the whole ant colony fitness is evident in two key aspects. Symbiont workers fed diets where urea was the only source of nitrogen exhibited lower survival rates, and the larvae they cared for showed impaired development, reduced survival, lower pupation and emergence rates, and small adult body sizes upon eclosion (Fig. 4). These results suggest the importance of symbiont-mediated nitrogen metabolism, which supports the overall fitness of the ant colony. We indeed observe that, in the presence of symbionts within the bacterial pouch, a greater proportion of nitrogen derived from urea was assimilated into the body tissues of both adults and larvae, with larvae exhibiting a higher rate of nitrogen assimilation (Supplementary Fig. 14). Genomic analysis and heavy nitrogen urea labeling experiments revealed that symbionts in the bacterial pouch recycle nitrogenous waste, such as urate or urea, and convert symbiont-recycled nitrogen in the form of essential and non-essential amino acids utilized by ant hosts (Figs. 5 and 6). Taken together, the conserved N-recycling and N-provisioning roles of symbionts in the bacterial pouch of *T. nigra*-group ants support the hypothesis that this nutritional symbiosis plays an important role in the exploitation of an N-limited dietary niche. Similar functions are observed in other herbivorous ants, such as the endosymbiont *Blochmannia* in *Camponotini*[25] and the multi-partite gut bacterial communities in *Cephalotes* ants[17], where symbionts improve nitrogen economies by recycling nitrogen and further fueling the synthesis of essential amino acids. Despite differences in the symbiotic microbes involved, these herbivorous ants with nitrogen-poor diets exhibit a functional convergence in the adaptive role of symbiosis for nitrogen acquisition. This reflects the

502 generality of such functional convergence across herbivorous ant species inhabiting N-
503 limited environments.

504 The specialized structure connecting the bacterial pouch to the Malpighian tubules
505 reinforces the proposed biological role of *Tokpelaia*. The nitrogen recycling activity by
506 *Tokpelaia* is likely mediated through the delivery of host-derived waste nitrogen via the
507 Malpighian tubules into the bacterial pouch, where *Tokpelaia* resides. Additionally, this
508 structure's connection to the gut facilitates the export of amino acids synthesized from
509 assimilated recycled nitrogen by *Tokpelaia* cells, which are then transported to the host
510 gut. The high abundance of nitrogen-recycling symbionts at the site of insect nitrogen
511 waste delivery via the Malpighian tubules is also observed in the *Cephalotes* system.
512 Positioned at the site of host nitrogen waste delivery[17, 48], *Ischyrobacter davidsoniae*
513 plays a central role in a collaborative nitrogen-recycling symbiosis[23]. These findings
514 highlight the critical role of specialized symbiotic structures in facilitating nitrogen
515 recycling in insects, where the spatial arrangement of symbionts near nitrogen waste
516 delivery sites enables efficient nutrient cycling and contributes to the overall ecological
517 success of the host.

518 During the metamorphosis of holometabolous insects, significant morphological
519 and physiological changes provide opportunities for symbiotic mutualisms to become
520 dissociated. A notable example is the bacterium *Acetobacter thailandicus*, which stably
521 colonizes the gut of Drosophila adults. While it does not enhance adult fitness, it
522 significantly increases larval fitness[65]. This pattern may reflect a broader trend in
523 holometabolous insects, where adults carry and transmit symbiotic bacteria that
524 primarily benefit larvae, even without direct advantages to the adults. In social insects,
525 such cross-stage symbiont benefits are more pronounced due to the close physical
526 association between adults and larvae and the capacity for trophallactic feeding of
527 symbiont-derived metabolites produced by adults. In the *T. nigra*-group ants,
528 specialized *Tokpelaia* symbionts present exclusively in adults, enhance colony-wide
529 nitrogen economies. Their contributions to larval nitrogen budgets promote larval
530 growth and development. This adult-specific symbiosis is likely sustained through the

trophallactic transfer of extracellular symbionts during the adult stage.

Our findings suggest that this sophisticated structural design enables a highly efficient nitrogen economy within the holobiont of *T. nigra*-group ants. The strict compartmentalization of these structures stabilizes the symbiotic relationship by allowing the ant hosts to deliver precursors of the uricolytic pathway directly to the bacterial pouch. The symbionts, which reside within this structure, import uric acid and produce metabolites that are beneficial to the ants, functioning as "nutrient factories". These symbiont-derived metabolites are then distributed to colony members, particularly larvae that lack these symbionts, via trophallaxis, ensuring that the entire colony benefits from the nutritional symbiosis. This study enhances our understanding of insect-microbe symbioses, particularly in social insects, by adding the *T. nigra*-group ants to the list of species with well-characterized, specialized microbial associations. The findings highlight the importance of spatial organization in symbiotic systems, where specialized organs facilitate nutrient recycling and support host fitness. This work also provides new insights into nitrogen acquisition strategies in other herbivorous insects, like *Cephalotes* and *Camponotus* ants, where convergent symbiotic mechanisms may help overcome nitrogen limitations[17, 25]. Ultimately, this research opens avenues for further exploration of microbial co-diversification and the functional roles of symbioses in host evolution.

Methods

Ant collection and specimen identification

We collected 53 *Tetraponera* colonies from southern provinces of China, including Yunnan, Guangdong, and Jiangxi, between 2019 and 2024 (Supplementary Data 1). For molecular analysis, multiple workers were preserved in anhydrous ethanol and stored at -20°C before DNA extraction. Colonies designated for dietary manipulation experiments or microscopic observation were kept alive for laboratory rearing.

For identification, one individual from each colony was photographed and

558 classified based on morphology. Additionally, we selected another individual per
559 colony for DNA barcoding of the mitochondrial cytochrome oxidase I gene (COI) to
560 refine species identification, with COI sequences >600 bp unambiguously matched to
561 *Tetraponera* species in GenBank and BOLD database[66] included as a taxonomic
562 reference. Using the COI sequence of *Pseudomyrmex gracilis* (FJ436821.1), a sister
563 genus of *Tetraponera*, as an outgroup, we aligned all sequences with MAFFT v7.520[67]
564 and removed divergent or ambiguously aligned regions using Gblocks v0.91b[68].
565 Phylogenetic analyses were conducted using RAxML v8.2.12[69] with 1000 bootstrap
566 replicates under the GTRGAMMA model, and the resulting phylogeny was visualized
567 using iTOL[70]. Species delimitation was further assessed using the Automatic Barcode
568 Gap Discovery (ABGD) method[71], which detects barcode gaps by assuming non-
569 overlapping intra- and interspecific genetic distances. Pairwise K2P distance matrices
570 were calculated from the COI alignment (excluding the outgroup) using MEGA
571 v11.0.13[72]. These matrices were used for ABGD analysis performed online, with a
572 relative gap width (X) of 1.5, and results recorded for intraspecific divergence (P)
573 ranging from 0.001 to 0.1 (Supplementary Fig. 1).
574

575 **Trophic levels of *Tetraponera* ants determined by nitrogen isotope**
576 **ratios**

577 While collecting *Tetraponera* ants, we also gathered local plants, herbivores, and
578 predatory arthropods (Supplementary Data 2). To prevent contamination from residual
579 food in arthropod guts, we removed ant abdominal segments (gasters) before isotopic
580 analysis. Plant leaves and arthropod samples were dried using a vacuum-freeze dryer,
581 then ground for $\delta^{15}N$ analysis using a Delta A Advantage isotope ratio mass
582 spectrometer coupled with an EA-HT elemental analyzer (Thermo Fisher Scientific Inc.,
583 Bremen, Germany). The nitrogen isotope ratios expressed as $\delta^{15}N$ value was calculated
584 according to the equation: δ(‰) = [(Rsample - Rstandard)/Rstandard]*1000, where
585 Rsample is the $^{15}N/^{14}N$ ratio of the sample and Rstandard is the $^{15}N/^{14}N$ ratio of
586 atmospheric N_2 (Rstandard = 0.003676). To conduct comparisons across different

587 locations, we computed the average $\delta^{15}N$ values for plants ($\delta^{15}N$ plant) examined at
588 each specific site. The relative trophic level of ants and arthropods was then determined
589 by subtracting $\delta^{15}N$ plant from $\delta^{15}N$ ant/arthropod at each location. Finally, we adjusted
590 for local variation by subtracting the median $\delta^{15}N$ value of plants at each site from the
591 overall median value across all locations.

592 Microscopic analysis of bacterial pouch structure and symbiont 593 localization in *T. nigra*-group ants

594 To explore the organization of the bacterial pouch across different life stages in *T.*
595 *nigra*-group ants, we examined the gut structure of workers, pupae, and larvae of *T.*
596 *attenuata* using scanning electron microscopy (SEM). Guts were dissected and fixed
597 overnight at 4°C in 2.5% glutaraldehyde, followed by dehydration through a graded
598 ethanol series and drying using a critical point dryer (Leica CPD300). After sputter-
599 coating with gold (Hitachi E-1045), the samples were observed under an SEM (Hitachi
600 SU8010, Tokyo, Japan).

601 Fluorescence in situ hybridization (FISH) was then used to localize the symbiotic
602 bacteria in workers from four *T. nigra*-group species, following a previously published
603 protocol[49] Łukasik et al. (2017). Guts were dissected, fixed in 4% formaldehyde in PBS
604 at room temperature for 2 hours, and treated with 80% ethanol and 6% hydrogen
605 peroxide for 1–4 weeks to reduce autofluorescence. The samples were then rehydrated
606 by washing with PBSTx (PBS with 0.3% TritonX-100) for 10 minutes three times,
607 followed by washing with hybridization buffer (30% formamide, 0.01% SDS, 0.9 M
608 NaCl, and 0.02 M Tris-HCl, pH 8.0) for 10 minutes three times. Finally, samples were
609 incubated overnight at room temperature in a hybridization buffer containing 100 nM
610 EUB338 universal bacterial probe and 1% DAPI. After washing the specimens three
611 times for 10 minutes each with PBSTx, specimens were imaged using an inverted
612 fluorescence microscope (Observer Z1, Zeiss, Germany). To further identify specific
613 symbionts, a second round of FISH was performed using species-specific probes
614 targeting Hyphomicrobiales, including RHIZ1244[73] (Cy5-

615 TCGCTGCCCACTGTCACC) for *T. attenuata* and *T.* sp2, TBIRHI (Cy5-
616 TCGCTACCCACTGTCACC) for *T. binghami*, and TSP1RHI (Cy5-
617 TCGCTACCCATTGTCACC) for *T.* sp1.

618 To obtain detailed structure information on the bacterial pouch and associated
619 bacteria, we used transmission electron microscopy (TEM). Guts of *T. attenuata* were
620 dissected and fixed overnight in 2.5% glutaraldehyde in PBS at 4°C. After washing with
621 PBS four times, the samples were postfixed with 1% (w/v) osmium tetroxide in 0.1 M
622 PBS for 2h at room temperature. Then, the samples were dehydrated in a graded ethanol
623 series and then in pure acetone for 10 minutes twice. Then, the samples were infiltrated
624 in a graded mixture (3:1, 1:1, 1:3) of acetone and SPI-PON812 resin (16.2 g SPI-
625 PON812, 10 g DDSA and 8.9 g NMA) and then infiltrated in pure resin. Finally, tissues
626 were embedded in pure resin with 1.5% BDMA and polymerized at 45°C for 12h and
627 then at 60°C for 48 h. The ultrathin sections (70nm thick) were sectioned
628 with microtome (Leica EM UC6), double-stained by uranyl acetate and lead citrate, and
629 examined under a transmission electron microscope (Tecnai Spirit120kV, FEI, USA).

630 Bacterial 16S rRNA amplicon sequencing

631 We investigated the microbial community diversity of *T. nigra*-group ants through
632 the V4 region of the 16S rRNA amplicon sequencing. For each species, samples were
633 collected from 4-6 colonies, with 3-5 workers sampled per colony. The gaster of a single
634 worker ant was dissected using sterile forceps, and total genomic DNA was extracted
635 from each gaster using the DNeasy Blood and Tissue Kit (Qiagen, Germany), following
636 the manufacturer's protocol for Gram-positive bacteria. DNA was submitted to Beijing
637 Novogene Bioinformatics Technology Co., Ltd for amplicon library preparation. Along
638 with insect DNA samples, blank samples in our DNA extraction batches were included
639 to monitor potential contamination during sample preparation and sequencing. Pooled
640 libraries were sequenced on the Illumina NovaSeq6000 SP platform, generating
641 2x250bp reads (Supplementary Data 3).

642 The raw reads were demultiplexed, trimmed barcodes and primers, and merged
643 reads using FLASH v1.2.7[74]. Quality filtering was done with fastp v0.23.4[75], and

644 downstream analysis was performed using a modified version of the
645 "modified_LSD.py" script[76] from
646 https://github.com/catesval/army_ant_myrmecophiles. We made changes to the
647 database in the script to suit our requirements. Briefly, low-quality sequences were
648 removed using vsearch-2.15.2[77], followed by chimera removal and denoising with
649 usearch11.0.667[78], which produced zOTU abundance tables. zOTUs were clustered
650 into OTUs based on 97% similarity using the -cluster_otus and -uparseout parameters
651 in usearch, and the resulting clusters were checked for chimeras. Species classification
652 was performed by comparing sequences against the RDP database
653 (http://www.drive5.com/sintax/rdp_16s_v18.fa.gz) using vsearch.

654 Bacterial DNA present in reagents and the environment can significantly impact
655 microbial community profiles, especially in samples with low template concentrations[79].
656 To eliminate potential contamination, we implemented several steps following
657 established criteria[49] . First, we performed BLASTn searches against the NCBI database
658 to assign taxonomy. Sequences identified as mitochondria, chloroplasts, Archaea,
659 Eukarya, or chimera were then removed from further analysis. Next, sequences
660 obtained from cloning amplification experiments (Accession numbers PQ549644-
661 PQ549668), specifically designed to identify bacterial species in the ant gut, were used
662 as reference sequences. zOTUs that perfectly matched these reference sequences were
663 initially added to the final zOTU list. The remaining zOTUs were then screened for
664 potential contamination. Contaminants were identified by comparing their relative
665 abundance in experimental libraries to that in blank libraries. Specifically, zOTUs with
666 a maximum relative abundance at least ten times greater in any experimental library
667 than in any blank library were considered non-contaminants. Those non-contaminant
668 zOTUs were added to the final zOTU list for further analysis (Supplementary Data 4).

669 **Metagenomics**

670 For each ant species, we dissected the gut tissues of 10 workers from the same
671 colony using sterile forceps and pooled them into a single sample. The extracted DNA

672 was then sent to Beijing Novogene Bioinformatics Technology Co., Ltd for library
673 preparation, followed by metagenomic sequencing on the Illumina NovaSeq 6000
674 platform. Quality trimming of raw reads was done with Trimmomatic-0.39[80], followed
675 by read quality checks using FastQC
676 v0.11.9(http://www.bioinformatics.babraham.ac.uk/projects/fastqc). The trimmed
677 reads were assembled with IDBA-UD 1.1.3[81] using k values of 20, 40, 60, 80, and 100,
678 and assembly statistics were calculated with QUAST-5.0.2[82] (Supplementary Table 2).
679 Scaffolds were uploaded to the Integrated Microbial Genomes with Microbiome
680 Samples Expert Review (IMG/M-ER) website for taxonomic classification and gene
681 annotation[83]. We focused on N metabolism by utilizing KEGG as references to
682 manually construct the pathways involved in the degradation of nitrogenous wastes and
683 the biosynthesis of amino acids (Supplementary Data 7). The bacterial community
684 composition of all metagenomes in this study was visualized by the Taxon-Annotated
685 GC Coverage plots, which were generated by mapping raw reads to classified scaffolds
686 using BWA 0.7.1[84] and employing custom scripts based on a previously published
687 method[85].

688 Metagenomic binning and genome-based phylogenetic analysis of 689 symbiotic Bacteria

690 In order to obtain the draft genomes of individual symbiont strains, we used the
691 metaWRAP pipeline[86] using CONCOCT, MaxBin, and metaBAT binning modules. The
692 draft genomes were refined with the bin_refinement module using ≥80% completeness
693 and ≤10% contamination. Few scaffolds belonging to these draft genomes are not
694 classified or not predicted to be present in the *T. nigra*-group ants. To improve accuracy,
695 scaffolds from seven draft genomes were compared against the NCBI database using
696 BLASTn and BLASTx with an e-value threshold of 10^{-6} and 70% identity. Scaffolds
697 with unexpected classification or their read coverage significantly deviates from that of
698 most scaffolds within their respective draft genomes were manually removed from the
699 binning datasets (Supplementary Data 5). Bin completeness and contamination were

700 assessed with CheckM[87] and the taxonomic assignment was performed using the
701 Genome Taxonomy Database with gtdbtk-2.1.1[88] (Supplementary Table 3).
702 We further performed genome-based phylogenetic analysis of symbiotic bacteria
703 in *T. nigra*-group ants using draft genomic data. OrthoFinder v2.5.5[89] was used to
704 identify single-copy orthologous genes. Amino acid sequences of these genes were
705 aligned with MAFFT v7.520, and divergent/ambiguous regions were removed using
706 Gblocks v0.91b. Alignments were concatenated for phylogenetic inference. Prottest
707 v3.4.2[90] was used to select the optimal amino acid substitution model. Phylogenetic
708 analysis was then performed with RAxML v8.2.12 using the best model and 1000
709 bootstrap replicates. Results were visualized and annotated on iTOL (Supplementary
710 Data 6).

711 Symbiont manipulation and ^{15}N-labeled urea feeding experiments

712 In order to perform symbiont manipulation experiments, we first obtained large
713 numbers of symbiont-free workers without the use of antibiotics. *T. attenuata* and *T.*
714 sp1 colonies were collected from Yunnan Province (Supplementary Data 1) and reared
715 on a diet of 30% honey water and mealworms at 25°C with a 14:10 light-dark cycle. A
716 fresh diet was provided every two days. To generate symbiont-free workers, pupae with
717 pigmented eyes were removed from the original cages and placed in sterile dishes.
718 Those pupae kept under sterile conditions will emerge as adult workers with no bacteria
719 in the bacterial pouch, confirmed by PCR amplification using both universal bacterial
720 and *Tokpelaia*-specific 16S rRNA gene primers, as well as whole-mount FISH staining
721 (Supplementary Fig. 11).
722 Controlled lab experiments were conducted on two ant species, *T. attenuata* and *T.*
723 sp1, to quantify the symbionts' contributions to the colony-wide nitrogen economy
724 through N recycling of dietary N waste (Supplementary Fig. 12). For each species, three
725 or four colonies were selected as biological replicates. Within each colony, individuals
726 were randomly assigned to one of the three treatments: (1) workers harboring symbiotic
727 bacteria in the bacterial pouch (Sym-worker), fed 30% sucrose water containing 1%
728 (w/v) ^{15}N-labeled urea; (2) workers without symbiotic bacteria in the bacterial pouch

(Apo-worker), fed the same ^{15}N-labeled urea solution; (3) workers with symbiotic bacteria in the bacterial pouch, fed 30% sucrose water containing 1% (w/v) ^{14}N-labeled urea as a control.

We initially conducted the ^{15}N-labeled urea feeding experiments exclusively with worker ants for 3 weeks. At the end of the experiment, hemolymph was collected from the surviving workers. Based on the number of remaining workers, we aimed to ensure 2–3 replicates for each treatment group within each colony (Supplementary Data 10). Hemolymph from each replicate was pooled to measure the enrichment of ^{15}N in amino acids within ant hemolymph at the Scale Biomedicine Technology Co., LTD (Beijing, China). Chromatographic separation of each hemolymph-water mixture was performed on Ultra-High Performance Liquid Chromatography (UHPLC)–High Resolution Tandem Mass Spectrometry (HRMS/MS).

Next, we extended the ^{15}N-labeled urea feeding experiments to include larvae tended by adult workers, with experimental durations of 30 days and 90 days. In the 30-day experiment, each treatment group was assigned 10 workers and 30 larvae. We recorded worker and larval survival throughout the whole period. In addition, we monitored larval growth and development by measuring larval body length daily. At the end of the experiment, the ^{15}N abundance in larval and worker body tissues, excluding the gut to avoid potential food contamination, was measured using a MAT253 stable isotope mass spectrometer at the Beijing Academy of Agriculture and Forestry Sciences (BAAFS) to determine whether the nitrogen assimilated from urea by symbiotic bacteria was utilized by the host and incorporated into its body tissues. At the same time, 3-5 larvae from each group were sent to Scale Biomedicine Technology Co., LTD (Beijing, China), where the relative abundance of ^{15}N-labeled amino acids was analyzed using UHPLC-HRMS/MS. In addition, we performed the 90-day experiment, with each group assigned 15 workers and 50 larvae, to record larval pupation and eclosion rates and measure the head width of newly emerged workers as an indicator of the worker body size. The detailed methods and statistical analysis can be found in the Supplementary Methods.

Acknowledgements

This study was supported by the National Natural Science Foundation of China 32370448 to Y. H., Beijing Advanced Innovation Program for Land Surface Science and the "111" Program of Introducing Talents of Discipline to Universities (B13008).

Data Availability

All data generated in this study are publicly available. The 16S amplicon sequencing data have been deposited in the GenBank Short Read Archive under BioProject PRJNA1159735, while the 16S rRNA sequences obtained via Sanger sequencing are accessible in GenBank under accession numbers PQ549644-PQ549668. Additionally, raw data from the stable isotope mass spectrometer and UHPLC-HRMS/MS are provided in the Supplementary Tables, and details on the PCR primers and FISH probes can be found in the Supplementary Tables and Methods.

References

1. Markmann, K. & Parniske, M. Evolution of root endosymbiosis with bacteria: how novel are nodules? *Trends Plant Sci.* **14**, 77-86 (2009).
2. Desbrosses, G. J. & Stougaard, J. Root nodulation: a paradigm for how plant-microbe symbiosis influences host developmental pathways. *Cell Host Microbe* **10**, 348-358 (2011).
3. McFall-Ngai, M. J. The importance of microbes in animal development: lessons from the squid-vibrio symbiosis. *Annu. Rev. Microbiol.* **68**, 177-194 (2014).
4. Belcaid, M., et al. Symbiotic organs shaped by distinct modes of genome evolution in cephalopods. *Proc. Natl. Acad. Sci. USA* **116**, 3030-3035 (2019).
5. Skelton, J., Johnson, A. J., Jusino, M. A., Bateman, C. C., Li, Y. & Hulcr, J. A selective fungal transport organ (mycangium) maintains coarse phylogenetic congruence between fungus-farming ambrosia beetles and their symbionts. *Proc. R. Soc. B* **286**, 20182127 (2019).
6. Goodchild, A. J. P. Studies on the functional anatomy of the intestines of Heteroptera. *Proceedings of the Zoological Society of London* **141**, 851-910 (1963).
7. Kuechler, S. M., Fukatsu, T. & Matsuura, Y. Repeated evolution of bacteriocytes in lygaeoid stinkbugs. *Environ. Microbiol.* **21**, 4378-4394 (2019).
8. Oishi, S., Moriyama, M., Koga, R. & Fukatsu, T. Morphogenesis and development of midgut symbiotic organ of the stinkbug *Plautia stali* (Hemiptera: Pentatomidae). *Zool. Lett.* **5**, 16-29 (2019).
9. Jackson, R., et al. Convergent evolution of a labile nutritional symbiosis in ants. *ISME J.* **16**, 2114-2122 (2022).

10. Russell, J. A., Sanders, J. G. & Moreau, C. S. Hotspots for symbiosis: function, evolution, and specificity of ant-microbe associations from trunk to tips of the ant phylogeny (Hymenoptera: Formicidae). *Myrmecological News* **24**, 43-69 (2017).
11. Russell, J. A., Moreau, C. S., Goldman-Huertas, B., Fujiwara, M. & Lohman, D. J. Bacterial gut symbionts are tightly linked with the evolution of herbivory in ants. *Proc. Natl. Acad. Sci. USA* **106**, 21236-21241 (2009).
12. Pringle, E. G. Convergence, constraint and the potential for mutualism between ants and gut microbes. *Mol. Ecol.* **28**, 699-702 (2019).
13. Sanders, J. G., et al. Dramatic differences in gut bacterial densities correlate with diet and habitat in rainforest ants. *Integr. Comp. Biol.* **57**, 705-722 (2017).
14. Klein, A., et al. A novel intracellular mutualistic bacterium in the invasive ant *Cardiocondyla obscurior*. *ISME J.* **10**, 376-388 (2016).
15. Neuvonen, M. M., et al. The genome of Rhizobiales bacteria in predatory ants reveals urease gene functions but no genes for nitrogen fixation. *Scientific Reports* **6**, 39197 (2016).
16. Bisch, G., et al. Genome evolution of Bartonellaceae symbionts of ants at the opposite ends of the trophic scale. *Genome Biol. Evol.* **10**, 1687-1704 (2018).
17. Hu, Y., et al. Herbivorous turtle ants obtain essential nutrients from a conserved nitrogen-recycling gut microbiome. *Nat. Commun.* **9**, 964-978 (2018).
18. Blüthgen, N., Gebauer, G. & Fiedler, K. Disentangling a rainforest food web using stable isotopes: dietary diversity in a species-rich ant community. *Oecologia* **137**, 426-435 (2003).
19. Davidson, D. W., Cook, S. C., Snelling, R. R. & Chua, T. H. Explaining the abundance of ants in lowland tropical rainforest canopies. *Science* **300**, 969-972 (2003).
20. Davidson, D. W. Ecological stoichiometry of ants in a New World rain forest. *Oecologia* **142**, 221-231 (2004).
21. Gil, R., et al. The genome sequence of *Blochmannia floridanus*: comparative analysis of reduced genomes. *Proc. Natl. Acad. Sci. USA* **100**, 9388-9393 (2003).
22. de Souza, D. J., Bézier, A., Depoix, D., Drezen, J. M. & Lenoir, A. *Blochmannia* endosymbionts improve colony growth and immune defence in the ant *Camponotus fellah*. *BMC Microbiol.* **9**, 29-37 (2009).
23. Béchade, B., et al. Physiological and evolutionary contexts of a new symbiotic species from the nitrogen-recycling gut community of turtle ants. *ISME J.* **17**, 1751-1764 (2023).
24. Csata, E. & Dussutour, A. Nutrient regulation in ants (Hymenoptera: Formicidae): a review. *Myrmecological News* **29**, 111-124 (2019).
25. Feldhaar, H., et al. Nutritional upgrading for omnivorous carpenter ants by the endosymbiont *Blochmannia*. *BMC Biol.* **5**, 48-59 (2007).
26. Ward, P. S. *Taxonomy, phylogeny and biogeography of the ant genus Tetraponera (Hymenoptera:Formicidae) in the Oriental and Australian regions*. Legare Street Press (2001).
27. Ward, P. S. The ant genus *Tetraponera* in the Afrotropical region: synopsis of species groups and revision of the *T. ambigua*-group (Hymenoptera: Formicidae). In: *Myrmecologische Nachrichten*). antbase.org (2006).
28. Chong, K. F. & Lee, C. Y. Inter- and intraspecific aggression in the invasive longlegged ant (Hymenoptera: Formicidae). *J. Econ. Entomol.* **103**, 1775-1783 (2010).
29. Wheeler, W. M. & Bailey, I. W. The feeding habits of Pseudomyrmine and other ants. *Transactions of the American Philosophical Society* **22**, 235-279 (1920).

30. Klein, R. W., Kovac, D., Schellerich, A. & Maschwitz, U. Mealybug-carrying by swarming queens of a southeast asian bamboo-inhabiting ant. *Naturwissenschaften* **79**, 422-423 (1992).
31. Billen, J. & Buschinger, A. Morphology and ultrastructure of a specialized bacterial pouch in the digestive tract of *Tetraponera* ants (Formicidae, Pseudomyrmecinae). *Arthropod Struct. Dev.* **29**, 259-266 (2000).
32. Salem, H., et al. Drastic genome reduction in an herbivore's pectinolytic symbiont. *Cell* **171**, 1520-1531 (2017).
33. Hosokawa, T., Imanishi, M., Koga, R. & Fukatsu, T. Diversity and evolution of bacterial symbionts in the gut symbiotic organ of jewel stinkbugs (Hemiptera: Scutelleridae). *Appl. Entomol. Zool.* **54**, 359-367 (2019).
34. Cook, S. C. & Davidson, D. W. Nutritional and functional biology of exudate-feeding ants. *Entomol. Exp. Appl.* **118**, 1-10 (2006).
35. Ward, P. S. Phylogenetic analysis of Pseudomyrmecine ants associated with domatia-bearing plants. In: *Ant-Plant Interactions* (eds Huxley CR, Cutler DF). Oxford University Press (1991).
36. Buschinger, A., Klein, R. W. & Maschwitz, U. Colony structure of a bamboo-dwelling *Tetraponera* sp. (Hymenoptera: Formicidae: Pseudomyrmecinae) from Malaysia. *Ins. Soc.* **41**, 29-41 (1994).
37. Braekman, J. C., et al. *Tetraponerine*-8, an alkaloidal contact poison in a Neoguinean Pseudomyrmecine ant, *Tetraponera* sp. *Zeitschrift für Naturforschung C* **42**, 627-630 (1987).
38. Midha, S., Rigden, D. J., Siozios, S., Hurst, G. D. D. & Jackson, A. P. *Bodo saltans* (Kinetoplastida) is dependent on a novel *Paracaedibacter*-like endosymbiont that possesses multiple putative toxin-antitoxin systems. *ISME J.* **15**, 1680-1694 (2021).
39. George, E. E., et al. Highly reduced genomes of protist endosymbionts show evolutionary convergence. *Curr. Biol.* **30**, 925-933 (2020).
40. Weinstock, O., Weinstock, O., Sella, C., Chipman, D. M. & Barak, Z. Properties of subcloned subunits of bacterial acetohydroxy acid synthases. *J Bacteriol.* **174**, 5560-5566 (1992).
41. Dittmer, J., Bredon, M., Moumen, B., Raimond, M., Grève, P. & Bouchon, D. The terrestrial isopod symbiont 'Candidatus Hepatincola porcellionum' is a potential nutrient scavenger related to Holosporales symbionts of protists. *ISME Commun.* **3**, 18-30 (2023).
42. Giovannini, M., Petroni, G. & Castelli, M. Novel evolutionary insights on the interactions of the Holosporales (Alphaproteobacteria) with eukaryotic hosts from comparative genomics. *Environ. Microbiol.* **26**, e16562 (2024).
43. Sauer, C., Dudaczek, D., Hölldobler, B. & Gross, R. Tissue localization of the endosymbiotic bacterium "*Candidatus* Blochmannia floridanus" in adults and larvae of the carpenter ant *Camponotus floridanus*. *Appl. Environ. Microbiol.* **68**, 4187-4193 (2002).
44. Ramalho, M. O., Vieira, A. S., Pereira, M. C., Moreau, C. S. & Bueno, O. C. Transovarian transmission of *Blochmannia* and *Wolbachia* endosymbionts in the Neotropical weaver ant *Camponotus textor* (Hymenoptera, Formicidae). *Curr. Microbiol.* **75**, 866-873 (2018).
45. Kwong, W. K. & Moran, N. A. Gut microbial communities of social bees. *Nat. Rev. Microbiol.* **14**, 374-384 (2016).
46. Moran, N. A., Hansen, A. K., Powell, J. E. & Sabree, Z. L. Distinctive gut microbiota of honey bees assessed using deep sampling from individual worker bees. *PLoS One* **7**, e36393 (2012).
47. Martinson, V. G., Danforth, B. N., Minckley, R. L., Rueppell, O., Tingek, S. & Moran, N. A. A simple and distinctive microbiota associated with honey bees and bumble bees. *Mol. Ecol.* **20**, 619-628 (2011).

48. Flynn, P. J., D'Amelio, C. L., Sanders, J. G., Russell, J. A. & Moreau, C. S. Localization of bacterial communities within gut compartments across *Cephalotes* turtle ants. *Appl. Environ. Microbiol.* **87**, e02803-02820 (2021).
49. Łukasik, P., et al. The structured diversity of specialized gut symbionts of the New World army ants. *Mol. Ecol.* **26**, 3808-3825 (2017).
50. Li, H., et al. Convergent evolution of complex structures for ant-bacterial defensive symbiosis in fungus-farming ants. *Proc. Natl. Acad. Sci. USA* **115**, 10720-10725 (2018).
51. Oishi, S., Moriyama, M., Mizutani, M., Futahashi, R. & Fukatsu, T. Regulation and remodeling of microbial symbiosis in insect metamorphosis. *Proc. Natl. Acad. Sci. USA* **120**, e2304879120 (2023).
52. Oguchi, K., Harumoto, T., Katsuno, T., Matsuura, Y., Chiyoda, S. & Fukatsu, T. Intracellularity, extracellularity, and squeezing in the symbiotic organ underpin nurturing and functioning of bacterial symbiont in leaf beetles. *iScience* **27**, 109731-109744 (2024).
53. Fronk, D. C. & Sachs, J. L. Symbiotic organs: the nexus of host-microbe evolution. *Trends Ecol. Evol.* **37**, 599-610 (2022).
54. González Porras, M. Á., et al. Extracellular symbiont colonizes insect during embryo development. *ISME Commun.* **4**, ycae005 (2024).
55. Nalepa, C. A. Origin of termite eusociality: trophallaxis integrates the social, nutritional, and microbial environments. *Ecol. Entomol.* **40**, 323-335 (2015).
56. Lanan, M. C., Rodrigues, P. A. R., Agellon, A., Jansma, P. & Wheeler, D. E. A bacterial filter protects and structures the gut microbiome of an insect. *ISME J.* **10**, 1866-1876 (2016).
57. Powell, J. E., Martinson, V. G., Urban-Mead, K., Moran, N. A. & Goodrich-Blair, H. Routes of acquisition of the gut microbiota of the honey bee *Apis mellifera*. *Appl. Environ. Microbiol.* **80**, 7378-7387 (2014).
58. Van Borm, S., Buschinger, A., Boomsma, J. J. & Billen, J. *Tetraponera* ants have gut symbionts related to nitrogen-fixing root-nodule bacteria. *Proc. R. Soc. Lond. B.* **269**, 2023-2027 (2002).
59. Stoll, S., Gadau, J., Gross, R. & Feldhaar, H. Bacterial microbiota associated with ants of the genus *Tetraponera*. *Biol. J. Linn. Soc.*, 399–412 (2007).
60. Salem, H. & Kaltenpoth, M. Beetle–bacterial symbioses: endless forms most functional. *Annu. Rev. Entomol.* **67**, 201-219 (2022).
61. Salem, H., et al. Symbiont digestive range reflects host plant breadth in herbivorous beetles. *Curr. Biol.* **30**, 2875-2886 (2020).
62. Brune, A. & Dietrich, C. The gut microbiota of termites: digesting the diversity in the light of ecology and evolution. *Annu. Rev. Microbiol.* **69**, 145-166 (2015).
63. Arora, J., et al. The functional evolution of termite gut microbiota. *Microbiome* **10**, 78-100 (2022).
64. Engel, P. & Moran, N. A. The gut microbiota of insects - diversity in structure and function. *FEMS Microbiol. Rev.* **37**, 699-735 (2013).
65. Pais, I. S., Valente, R. S., Sporniak, M. & Teixeira, L. *Drosophila melanogaster* establishes a species-specific mutualistic interaction with stable gut-colonizing bacteria. *PLoS Biol.* **16**, e2005710 (2018).
66. Ratnasingham, S. & Hebert, P. D. N. BOLD : the barcode of life data system. *Mol. Ecol. Notes* **7**, 355-364 (2007).
67. Rozewicki, J., Li, S., Amada, K. M., Standley, D. M. & Katoh, K. MAFFT-DASH: integrated protein sequence and structural alignment. *Nucleic Acids Res.* **47**, W5-W10 (2019).
68. Talavera, G. & Castresana, J. Improvement of phylogenies after removing divergent and ambiguously aligned blocks from protein sequence alignments. *Syst. Biol.* **56**, 564-577 (2007).

69. Stamatakis, A. RAxML version 8: a tool for phylogenetic analysis and post-analysis of large phylogenies. *Bioinformatics* **30**, 1312-1313 (2014).
70. Letunic, I. & Bork, P. Interactive Tree Of Life (iTOL) v5: an online tool for phylogenetic tree display and annotation. *Nucleic Acids Res.* **49**, W293-W296 (2021).
71. Puillandre, N., Lambert, A., Brouillet, S. & Achaz, G. ABGD, Automatic Barcode Gap Discovery for primary species delimitation. *Mol. Ecol.* **21**, 1864-1877 (2012).
72. Tamura, K., Stecher, G., Kumar, S. & Battistuzzi, F. U. MEGA11: molecular evolutionary genetics analysis version 11. *Mol. Biol. Evol.* **38**, 3022-3027 (2021).
73. Thayanukul, P., Zang, K., Janhom, T., Kurisu, F., Kasuga, I. & Furumai, H. Concentration-dependent response of estrone-degrading bacterial community in activated sludge analyzed by microautoradiography-fluorescence *in situ* hybridization. *Water Res.* **44**, 4878-4887 (2010).
74. Magoč, T. & Salzberg, S. L. FLASH: fast length adjustment of short reads to improve genome assemblies. *Bioinformatics* **27**, 2957-2963 (2011).
75. Chen, S. Ultrafast one-pass FASTQ data preprocessing, quality control, and deduplication using fastp. *iMeta* **2**, e107 (2023).
76. Valdivia, C., et al. Microbial symbionts are shared between ants and their associated beetles. *Environ. Microbiol.* **25**, 3466-3483 (2023).
77. Rognes, T., Flouri, T., Nichols, B., Quince, C. & Mahé, F. VSEARCH: a versatile open source tool for metagenomics. *PeerJ* **4**, e2584 (2016).
78. Edgar, R. C. Search and clustering orders of magnitude faster than BLAST. *Bioinformatics* **26**, 2460-2461 (2010).
79. Salter, S. J., et al. Reagent and laboratory contamination can critically impact sequence-based microbiome analyses. *BMC Biol.* **12**, 87-99 (2014).
80. Bolger, A. M., Lohse, M. & Usadel, B. Trimmomatic: a flexible trimmer for Illumina sequence data. *Bioinformatics* **30**, 2114-2120 (2014).
81. Peng, Y., Leung, H. C., Yiu, S. M. & Chin, F. Y. IDBA-UD: a de novo assembler for single-cell and metagenomic sequencing data with highly uneven depth. *Bioinformatics* **28**, 1420-1428 (2012).
82. Mikheenko, A., Prjibelski, A., Saveliev, V., Antipov, D. & Gurevich, A. Versatile genome assembly evaluation with QUAST-LG. *Bioinformatics* **34**, i142-i150 (2018).
83. Chen, I. M. A., et al. The IMG/M data management and analysis system v.7: content updates and new features. *Nucleic Acids Res.* **51**, D723-D732 (2023).
84. Li, H. & Durbin, R. Fast and accurate short read alignment with Burrows-Wheeler transform. *Bioinformatics* **25**, 1754-1760 (2009).
85. Kumar, S., Jones, M., Koutsovoulos, G., Clarke, M. & Blaxter, M. Blobology: exploring raw genome data for contaminants, symbionts and parasites using taxon-annotated GC-coverage plots. *Front Genet* **4**, 237-249 (2013).
86. Uritskiy, G. V., DiRuggiero, J. & Taylor, J. MetaWRAP—a flexible pipeline for genome-resolved metagenomic data analysis. *Microbiome* **6**, 158-171 (2018).
87. Parks, D. H., Imelfort, M., Skennerton, C. T., Hugenholtz, P. & Tyson, G. W. CheckM: assessing the quality of microbial genomes recovered from isolates, single cells, and metagenomes. *Genome Res.* **25**, 1043-1055 (2015).
88. Chaumeil, P. A., Mussig, A. J., Hugenholtz, P. & Parks, D. H. GTDB-Tk: a toolkit to classify genomes with the Genome Taxonomy Database. *Bioinformatics* **36**, 1925-1927 (2019).
89. Emms, D. M. & Kelly, S. OrthoFinder: solving fundamental biases in whole genome comparisons

968 dramatically improves orthogroup inference accuracy. *Genome Biology* **16**, 157-171 (2015).
969 90. Darriba, D., Taboada, G. L., Doallo, R. & Posada, D. ProtTest 3: fast selection of best-fit models of
970 protein evolution. *Bioinformatics* **27**, 1164-1165 (2011).
971
972